

1 Article

2 Silica Modified by Using Alcohol Polyoxyethylene 3 Ether and Silane Coupling Agent together to Achieve 4 High Performance Rubber Composites Using Latex 5 Compounding Method

6 Junchi Zheng ^b, Xin Ye ^b, Dongli Han ^b, Suhe Zhao, Xiaohui Wu ^b, Youping Wu ^{a,b}, Dong Dong
7 ^c, Yiqing Wang ^{a,b,*}, Liqun Zhang ^{a,b,*}

8 ^a State Key Laboratory of Organic-Inorganic Composites, Beijing University of Chemical Technology, Beijing
9 100029, PR China

10 ^b Engineering Research Center of Elastomer Materials on Energy Conservation and Resources, Ministry of
11 Education, Beijing 100029, PR China

12 ^c Red Avenue New Materials Group Co., Ltd, Shanghai 200120, PR China

13 * Corresponding author: E-mail address: zhanglq@mail.buct.edu.cn (L. Zhang). Address: P.O. Box 57, Beijing
14 University of Chemical Technology, Beisanhuan East Road, Beijing 100029, China;
15 Tel.: +86-13910215964; fax: +86-010-64443413.

16 **Abstract:** Nowadays, the study of preparing silica/rubber composites, which can be used in “green
17 tire”, in energy saving method is fast-growing. In our work, silica modified by using alcohol
18 polyoxyethylene ether (AEO) and 3-Mercaptopropyltriethoxysilane (K-MEPTS) together were
19 investigated. Thermal gravimetric analyzer (TGA) result indicated that both AEO and K-MEPTS
20 could be grafted on the silica surface. Raman spectroscopy confirmed that the AEO could generate
21 a certain steric hindrance for the mercaptopropyl group on K-MEPTS. Silica modified by using AEO
22 and K-MEPTS together can be completely co-coagulated with the rubber in preparing silica/natural
23 rubber (NR) composites by latex compounding method. AEO can form a physical interface between
24 silica and rubber; meanwhile, K-MEPTS can form a chemical interface between silica and rubber.
25 The effects of chemical and physical interface between silica and rubber on dynamic and mechanical
26 performances of silica/NR composites were also given in this research. A proper combination of
27 physical and chemical interface between silica and NR can improve performances of silica/NR
28 composites.

29 **Keywords:** chemical and physical interface; surface modification of silica; latex compounding
30 method; silica/NR composite
31

32 1. Introduction

33 Silica is a non-carbon filler that serves as an extremely important reinforcing filler in the rubber
34 industry [1]. Previous researchers have confirmed that silica could provide a combination of good
35 mechanical performances [2], high wet grip resistance [3], and low rolling resistance [4] for
36 silica/rubber composites. At present, silica/rubber composites are commonly used in producing the
37 tread of “green tire” [5,6].

38 As an inorganic particle, silica has huge amounts of hydroxyl groups (–OH) on its surface [7],
39 leading to the nature of the silica particle [8-10]. Therefore, silica particle is less compatible with a
40 hydrophobic polymer, such as rubber [11]. However, the silica surface is modifiable because of the
41 numerous reactive hydroxyl groups [12,13]. Silica modification is an effective way to improve the
42 compatibility between silica and rubber. Treatment with reactive silane coupling agent (SCA) is one
43 of the major methods in silica modification [14,15]. In principle, SCA possesses readily hydrolyzable
44 alkoxy group that can react with hydroxyl groups on the silica surface to form a stable siloxane
45 linkage [16]. Surface active agent (SAA) is another modifier that is commonly used in silica

46 modification. SAA can absorb on the silica surface, resulting in covering silica surface and reducing
47 the amount of hydroxyl groups exposed.

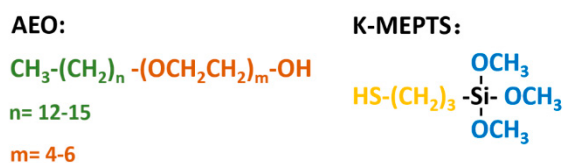
48 NR, which contains 93%–95% cis-1,4-polyisoprene, is an essential biosynthesized polymer [17].
49 It is naturally in the form of a colloidal system known as NR latex, in which rubber particles are
50 dispersed in an aqueous medium [18,19]. Therefore, the latex compounding method can be applied
51 in preparing silica/NR composites to solve the problems of low efficiency and high pollution in the
52 outdated mechanical blending method [20,21].

53 The key to the latex compounding method is to make sure that the silica can be completely co-
54 coagulated with the rubber. What's more, the performance of silica/rubber composites is determined
55 by the silica dispersion and the interface between silica and rubber. Thus, preparing a modified silica
56 with an ideal organic surface is important for preparing high performance silica/rubber composites
57 by latex compounding method.

58 In previous research, silica/rubber masterbatches had been prepared by latex compounding
59 method [21-24]. Various sulfide containing SCAs had been used for silica modification in these
60 preparations. The dispersion of silica in aqueous phase was improved by the help of sulfide-
61 containing SCA. Moreover, the sulfide-containing SCA could form "coupling bridge" [25], which was
62 a typical chemical interface between silica and rubber, resulting in improving the dynamic
63 performances of silica/rubber composites [26]. The essence of silica modified by SCA in the aqueous
64 phase is that the hydroxyl groups on the silica react with the hydroxyl groups of hydrolysates of SCA
65 [27]. The polycondensation also occurs among the hydroxyl groups of hydrolysates of SCA,
66 producing the polycondensates of SCA, which results in the aggregation of several SCA molecules
67 [28]. Therefore, using SCA only in silica modification is not efficient enough to improve the dispersion
68 of silica. Meanwhile, only chemical interface existing between silica and rubber is detrimental to the
69 stretching of rubber molecular chain under external force [29-31]. Moreover, the reaction between
70 rubber and sulfide-containing SCA ("scorchy" behavior) is inevitable during the process [32], even
71 though the mixing time and temperature are precisely controlled. Therefore, utilizing sulfide-
72 containing SCA only in silica modification for preparing silica/rubber composites is not the ideal
73 method.

74 SAA could modify silica directly in the aqueous phase without polycondensation, and most of
75 SAA had no react with rubber under any conditions. Therefore, only physical interface between silica
76 and rubber can be formed by the help of SAA [33-35]. However, dynamic performance of
77 silica/rubber composites is very poor in the absence of chemical interface between silica and rubber
78 [8,29]. Meanwhile, in our previous research, silica modified by SAA can not be completely co-
79 coagulated with the rubber in preparing silica rubber masterbatches by latex compounding method.

80 In this research, the silica/NR masterbatches, which was a floc containing silica and rubber, were
81 prepared by latex compounding method. Alcohol polyoxyethylene ether (AEO) [36] (as presented in
82 Fig. 1), which was a widely used nonionic SAA, and 3-Mercaptopropyltriethoxysilane (K-MEPTS)
83 [37] (as presented in Fig. 1), which had been commercially developed and widely used in the rubber
84 industry, were selected as modifiers to use together in silica modification in aqueous phase. This
85 method was rarely mentioned by previous researchers. The magnitude of chemical and physical
86 interface between silica and rubber could be varied by adjusting the amount of AEO and K-MEPTS
87 used in silica modification. The performances of silica/NR composites, which contained different
88 ratios of AEO and K-MEPTS, were compared. The effects of chemical and physical interface between
89 silica and rubber on different performance of silica/NR composites were also shown in this
90 comparison. Furthermore, the interaction between AEO and K-MEPTS also played an important role
91 in the preparation of silica/NR composites. The effect of this interaction on silica modification and
92 preparation of silica masterbatches and composites was introduced in this research.



93

94

Fig. 1 Chemical structure of AEO and K-MEPTS

95 **2. Experimental**96 *2.1. Materials*

97 High-ammonia NR latex with 60% total solid content was purchased from Hainan Rubber
 98 Industry Group Co., Ltd. (China). Precipitated silica water slurry of K-160 (nanoparticle size: 20–30
 99 nm, BET specific surface: 160.06 m²/g) was produced by Wilmar China (Jiamusi, China). AEO
 100 (average molecular weight: 421) was provided by Usolf. K-MEPTS (molecular weight: 196) was
 101 obtained from Nanjing Capatue Chemical Co., Ltd. (China). The rest of the required materials were
 102 commercially available.

103 *2.2. Preparation of modified silica*

104 Water was added into the precipitated silica slurry, and the solid content of silica slurry was
 105 measured to dilute to the 10% concentration. The silica water slurry was conducted under high-speed
 106 stirring for 30 min to obtain a stable suspension. Five beakers, numbered 1–5, were prepared, and
 107 1000 g of silica slurry was transferred to each beaker. The temperatures of all silica water slurry were
 108 heated to 70 °C under stirring. K-MEPTS (6, 6, 4, and 2 g) was added into beakers 1–4, and AEO (4, 6,
 109 8, and 8 g) was added into beakers 2–5, respectively. The slurry was stirred for 0.5 h, and the modified
 110 silica slurry was then obtained. According to the amount of AEO and K-MEPTS added in silica
 111 modification, we named the modified silica in beakers 1–5 as A0K6-MS, A4K6-MS, A6K4-MS, A8K2-
 112 MS, and A8K0-MS, respectively. The amounts of KH590 and AEO used in different modified silica
 113 are listed in Table 1.

114 Table 1 Formulation of modified silica and its name

Materials	A0K6-MS	A4K6-MS	A6K4-MS	A8K2-MS	A8K0-MS
Silica (dry weight) /g	100	100	100	100	100
K-MEPTS /g	6	6	4	2	0
AEO /g	0	4	6	8	8

115 *2.3. Preparation of masterbatches*

116 The modified silica slurry was cooled to room temperature and blended with the NR latex. The
 117 solid content of the NR latex was confirmed in advance, and the weight ratio of silica to NR was
 118 50:100 (e.g., 50 g of silica nanoparticles for every 100 g solid content of NR). Then, mixture of silica
 119 and NR latex was stirred for 0.5 h and coagulated with 3% formic acid solution. Finally, the flocs were
 120 washed with water six times and then dehydrated in a drying oven at 60 °C for 36 h to obtain
 121 silica/NR masterbatches. The masterbatches compounded with A0K6-MS, A4K6-MS, A6K4-MS,
 122 A8K2-MS, and A8K0-MS in preparation was named A0K6-MB, A4K6-MB, A6K4-MB, A8K2-MB, and
 123 A8K0-MB, respectively.

124 *2.4. Preparation of silica/NR composites*

125 The formulation of silica/NR compounds is demonstrated in Table 2. Silica/NR compounds were
 126 obtained by three stages of mixing. First, the masterbatches were masticated in an internal mixer

127 equipped with an oil circulating system to keep the processing temperature at 55 °C. Then, zinc oxide,
 128 stearic acid, and *N*-1,3-dimethylbutyl-*N'*-phenyl-*p*-phenylenediamine were added to the
 129 masterbatches successively. Second, compounds were kneaded for 5 min in the same internal mixer
 130 at 150 °C and then naturally cooled down to room temperature. Finally, *N*-cyclohexyl-2-
 131 benzothiazole-sulfenamide, diphenyl guanidine, and sulfur were uniformly blended in sequence
 132 with the cooled compound on a 6-inch mill (Shanghai Rubber Machinery Works No. 1, China) under
 133 room temperature. The total mixing time was kept not more than 15 min. The silica/NR compounds
 134 that contain A4K6-MB, A6K4-MB, and A8K2-MB are denoted as A4K6-C, A6K4-C, and A8K2-C,
 135 respectively.

136 Table 2 Formulation of silica/NR compounds

Materials	Amount (phr ^a)
Masterbatches	155
Stearic acid	2.0
Zinc oxide	5.0
<i>N</i> -1,3-dimethylbutyl- <i>N'</i> -phenyl- <i>p</i> -phenylenediamine	2.0
<i>N</i> -Cyclohexyl-2-benzothiazole sulfenamide	2.0
1,3-Diphenylguanidine	1.0
Sulfur	2.0

137 ^a parts per hundred of rubber.

138 The scorch time (T_{10}) and optimum cure time (T_{90}) of the compound were measured using disc
 139 vulkometer. The compounds were vulcanized at 143 °C according to their optimum cure time (T_{90}) in
 140 a standard mold to produce the silica/NR vulcanizates, which were stored at room temperature for
 141 at least 24 h before determining the performances.

142 2.5. Characterizations

143 The groups on pure and modified silica was characterized by Fourier transform infrared
 144 spectroscopy (FT-IR; Bruker Optik GmbH Co, Tensor 27, Germany), using the absorption mode
 145 under a wave number ranging from 4,000 cm^{-1} to 400 cm^{-1} with a resolution of 4 cm^{-1} . The samples
 146 were pressed into pellets together with potassium bromide.

147 Raman measurements were obtained using a Renishaw in Via Confocal Raman spectrometer
 148 (Gloucestershire, UK) coupled to a DMLM Leica microscope. The laser excitation wavelength is 514
 149 nm. The power of 514 nm argon ion excitation laser at the source is approximately 50 mW, and 20
 150 mW (highest power) at the surface of the sample. The Raman spectra of the samples were obtained
 151 from pressed solid samples in a sealed capillary tube.

152 Weight losses measurements of pure and modified silica and the masterbatches were performed
 153 on a thermal gravimetric analyzer (TGA) STARE system (Mettler-Toledo Co., Switzerland) under
 154 nitrogen atmosphere. Samples for TGA tests were heated at a heating rate of 10 °C/min. The residual
 155 weight of masterbatches, NR, silica, K-MEPTS and AEO were recorded as R_m , R_r , R_s , R_5 and R_A ,
 156 respectively.

157 The filler dispersion in silica/NR masterbatches and silica/NR composites were observed under
 158 a Tecnai G2 20 transmission electron microscope (TEM FEI Co., USA) with an accelerating voltage of
 159 200 kV. Thin sections for TEM observations were cut by a microtome at -100 °C and collected on
 160 copper grids.

161 The dynamic rheological performances of silica/NR compounds and silica/NR composites were
 162 analyzed using RPA2000 (Alpha Technologies Co., USA) at 60 °C. For the rubber compounds, the
 163 strain varied from 0.1% to 400% at the test frequency of 1 Hz. For the rubber vulcanizates, the strain
 164 varied from 0.1% to 40% at the test frequency of 1 Hz. The test of each specimen was repeated 3 times.

165 The vulcanization characteristics of silica/NR compounds were measured at 143°C by a P3555B2
 166 disc vulkometer (Beijing Huanfeng Chemical Machinery Trial Plant, China). The test of each
 167 specimen was repeated 3 times.

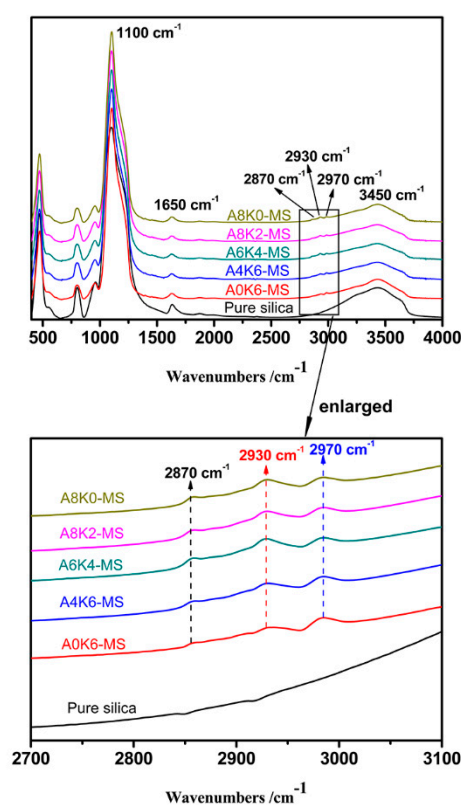
168 The mechanical performances of the silica/NR composites were investigated according to ASTM
 169 D638 specifications using a CMT4104 electrical tensile tester (Shenzhen SANS Test Machine Co.,
 170 China) with across head speed of 500 mm/min. The test of each specimen was repeated 5 times.

171 3. Results and discussion

172 3.1. Characterization of silica modified by AEO and K-MEPTS

173 3.1.1 FT-IR of pure and modified silica

174 As shown in Fig. 2, compared with the FT-IR spectra of the pure silica, all curves of the modified
 175 silica have absorption peaks at 2930 cm⁻¹, 2970 cm⁻¹ and 2870 cm⁻¹, which is attributed to vibrations
 176 of -CH₂- and -CH₃ bonds [38]. The appearance of organic groups, such as -CH₂- and -CH₃, on the
 177 modified silica surface shows that K-MEPTS and AEO exist on the silica surface.



178

179

Fig. 2 FT-IR spectra of pure silica and all modified silica

180 The absorption peaks at 3450 cm⁻¹ and 1650 cm⁻¹ correspond to the stretching and deforming
 181 vibration modes of the -O-H bonds [39], respectively. The relative intensity (RI) of the peak at 3400
 182 cm⁻¹ is determined by the number of -O-H bonds; therefore, a high RI means a large amount of
 183 hydroxyl groups on the silica surface. RI can be calculated by using the normalized FT-IR data, and
 184 the RI of all samples are listed in Table 3. The total weight of modifier used in the silica modification
 185 is equal for A4K6-MS, A6K4-MS and A8K2-MS, but the RI decreases sequentially. Therefore, AEO is
 186 a more effective modifier than K-MEPTS in changing the hydrophilicity of silica. This result could be
 187 attributed to the structure of AEO molecule, which was likely to cover multiple hydroxyl groups on
 188 the silica surface. In contrast, a K-MEPTS molecule could react with up to one hydroxyl group on the
 189 silica surface. The decrease in the hydrophilic nature of silica generally means that the dispersion of

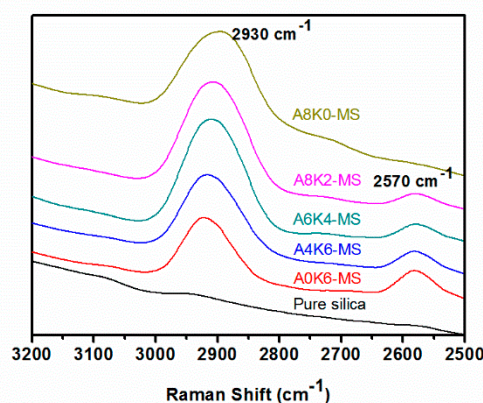
190 silica in aqueous phase is improved. Therefore, silica modified by using AEO and K-MEPTS together
 191 is an effective method in improving silica dispersion in aqueous phase, which is one of the key for
 192 preparing high performance silica/NR composites by latex compounding method.

193 Table 3 RI of the peak at 3400 cm^{-1} for pure silica and all modified silica

Samples	Pure silica	A0K6-MS	A4K6-MS	A6K4-MS	A8K2-MS	A8K0-MS
RI	0.318	0.211	0.189	0.184	0.178	0.196

194 3.1.2 Raman spectroscopy of pure and modified silica

195 Fig. 3 shows no peak on the curve of pure silica; therefore, no organic groups presents on the
 196 surface of pure silica. Meanwhile, Fig. 3 shows one peak on the curve of A8K0-MS and two peaks on
 197 others curve. The peak at 2930 cm^{-1} corresponds to methylene bonds, demonstrating that the AEO
 198 and K-MEPTS were grafted on the silica surface. Another peak is recorded at 2570 cm^{-1} , which
 199 corresponds to -S-H bonds, indicating that K-MEPTS was grafted on the silica surface.



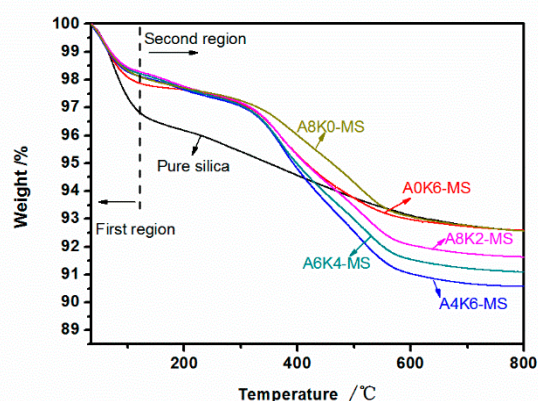
200

201 Fig. 3 Raman spectra of pure silica and all modified silica

202 The peak intensity around 2570 cm^{-1} for A4K6-MS is significantly weaker than that of A0K6-MS.
 203 The only difference for A0K6-MS and A4K6-MS was whether AEO should be utilized in silica
 204 modification. The most probable reason for this result was that AEO could generate a certain steric
 205 hindrance for the mercaptopropyl group on K-MEPTS.

206 3.1.3 TGA curves of pure and modified silica

207 As illustrated in Fig. 4 and Table 4, all the samples exhibit large weight losses in the region
 208 between 35°C and 120°C (first region). The weight loss in this region was caused by the removal of
 209 the adsorbed water. In a word, the amount of adsorbed water on the silica surface shows the same
 210 tendency as the amount of hydroxyl groups on the silica surface.



211

212

Fig. 4 TGA curves of pure silica and all modified silica

213 All of modified silica present a large weight loss in the region between 120°C and 800°C (second
 214 region). The weight loss of modified silica was due to the degradation of AEO and K-MEPTS, and
 215 the weight loss of pure silica was due to the dehydroxylation of hydroxyl groups. All modified silica
 216 has a larger weight loss than pure silica in the second region; meanwhile, A4K6-MS also has a larger
 217 weight loss than A0K6-MS in the second region. This is a noteworthy evidence, which indicates that
 218 both K-MEPTS and AEO were grafted on the silica surface.

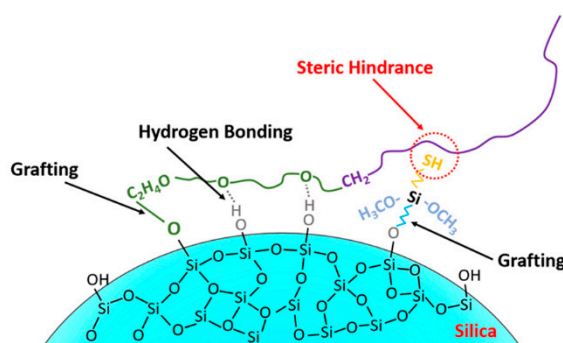
219

Table 4 Weight losses of pure and modified silica in the first and second regions

Samples	Weight loss in the first region (35°C –120°C) /%	Weight loss in the second region (120°C –800°C) /%
Pure silica	3.16	4.27
A0K6-MS	2.13	5.31
A4K6-MS	1.88	7.54
A6K4-MS	1.78	7.13
A8K2-MS	1.71	6.66
A8K0-MS	1.90	5.55

220 3.1.4 Schematic diagram of modifiers on the silica surface

221 The interaction between AEO and K-MEPTS is shown in Fig. 5 based on the above results. The
 222 activity of the mercaptopropyl on K-MEPTS would be affected by this interaction. Therefore, the
 223 chargeability and reactivity of silica modified by using AEO and K-MEPTS together differ from that
 224 of silica modified by using K-MEPTS only.



225

226

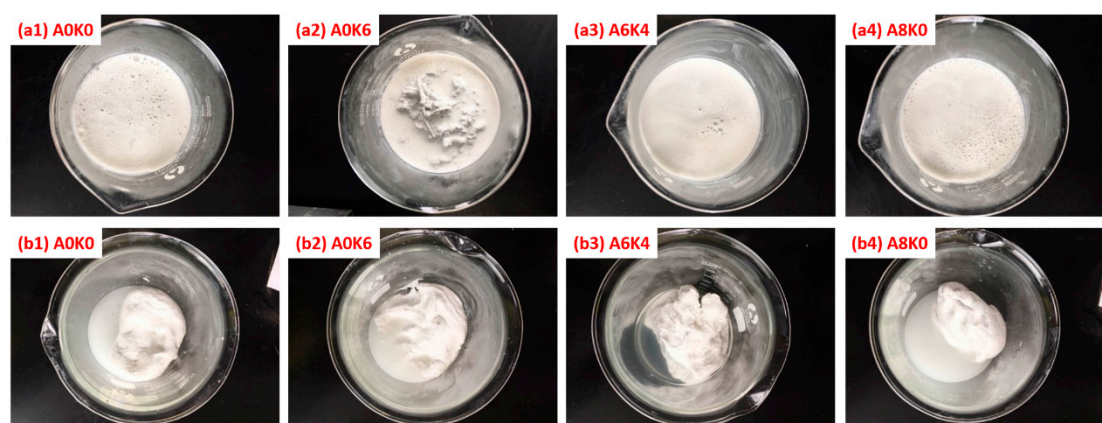
Fig. 5 Schematic diagram of the interaction between AEO and K-MEPTS in silica modification

227

228 3.2 Characterization of silica/NR masterbatches prepared by pure silica and modified silica

229 3.2.1. Co-coagulation of silica/NR mixture in preparing the masterbatches

230 The co-coagulation of silica/NR mixture in preparing the masterbatches by use of several
231 modified silica and pure silica (A0K0-MS) are shown in Fig. 6. Images of silica/NR mixtures, which
232 are prepared by adding the NR latex into the silica slurries and stirring for 10 minutes, are shown in
233 Fig. 6 (a). Images of masterbatches, which are prepared by adding the 3% formic acid solution into
234 mixtures, are shown in Fig. 6 (b). A6K4-MS is selected as representative for silica modified by using
235 AEO and K-MEPTS together, because the phenomenon in preparing silica/rubber masterbatches is
236 almost the same for A4K6-MS, A6K4-MS and A8K2-MS.

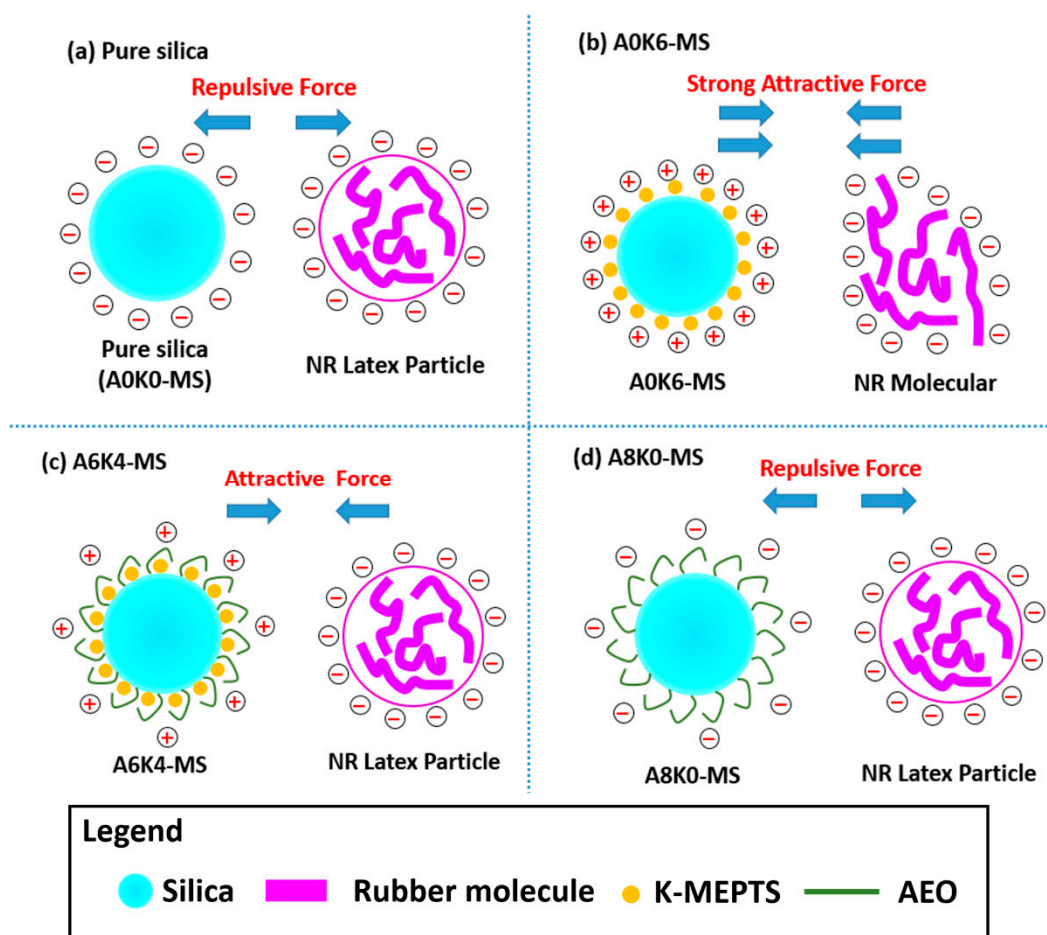


237

238 **Fig. 6** Preparation process of the masterbatches with pure and modified silica

239 As presented in Fig. 6 (a2), part of the mixture was coagulated when NR was mixed with A0K6-
240 MS, even if the formic acid solution was not added into this mixture. This phenomenon indicates that
241 K-MEPTS can promote the coagulation of NR latex. As presented in Fig. 6(b), A0K6-MB, A8K0-MB,
242 and pure silica masterbatch are largely clustered, and the residual aqueous phase is white and turbid
243 with abundant silica. Conversely, A6K4-MB is coagulated as complete sediments, and the residual
244 aqueous phase is clear.

245 The difference in coagulation phenomenon in different masterbatches was caused by
246 electrostatic attractive or repulsive force as presented in Fig. 7. The surface of both silica particle and
247 NR latex particle were negatively charged, causing an electrostatic repulsion in a system, as presented
248 in Fig. 7(a) [40]. Therefore, pure silica/NR masterbatch had a huge amount of silica loss in the aqueous
249 phase. K-MEPTS was positively charged, and its electronegativity contributed to the charge
250 neutralization of silica particles. The changes in the silica surface charge contributed to the adsorption
251 between rubber and silica. However, excessive K-MEPTS could result in significant positive charge
252 on the silica surface. Therefore, a strong attractive forces between silica particles and rubber latex
253 particles would damage the electrical layer stability of the rubber latex particles, which was destroyed
254 in this condition, as shown in Fig. 7(b). Therefore, mixture that consisted of A0K6-MS and NR latex
255 was coagulated in the absence of formic acid solution.



256

257

Fig. 7 Schematic diagram of the electrostatic force between pure or modified silica and NR

258 The positive charge of K-MEPTS, which was grafted on the silica surface, was weakened by the
 259 help of steric hindrance generated by AEO. Therefore, the attractive force between the NR latex
 260 particles and modified silica was adjusted to the appropriate level. Thus, A6K4-MB was successfully
 261 prepared. However, AEO was a nonionic surfactant that had no effect on the electrical performance
 262 of the silica surface. Therefore, a repulsive force still existed between A8K0-MS and NR latex particles,
 263 as presented in Fig. 7(d). In this condition, the co-coagulation of mixture latex, which consisted of NR
 264 latex and A8K0-MS, was unsatisfactory.

265

266 3.2.2 Actual amount of silica in silica/NR masterbatches

267 Table 5 Weight losses of six kinds of silica/NR masterbatches

Samples	Weight residual /%	Theoretical amount of silica in masterbatches /phr	Actual amount of silica in masterbatches /phr
Pure NR	1.32	-	-
Pure silica	92.57	-	-
KH-590	9.13	-	-
AEO	3.27	-	-
A0K6-MB	26.32	50	38.33
A4K6-MB	30.76	50	49.55
A6K4-MB	30.83	50	49.83
A8K2-MB	30.65	50	49.46
A8K0-MB	23.71	50	33.31
A0K0-MB	22.89	50	30.96

268 The actual amount of silica in the masterbatches are calculated using the following equation:
269

$$\text{Silica content (phr)} = \frac{100 \times (R_m - R_r)}{R_s + S_A \times R_A + S_5 \times R_5 - (1 + S_5 + S_A) \times R_m} \quad (1)$$

270 where R_m , R_r , R_s , R_5 and R_A are the 800°C weight (%) of masterbatches, rubber, silica, K-MEPTS and
271 AEO, respectively. S_5 is the weight ratio of K-MEPTS to modified silica and S_A is the weight ratio of
272 AEO to modified silica. The calculated results according to this equation are shown in Table 5. For all
273 masterbatches that contain silica modified by using K-MEPTS and AEO together, the actual amount
274 of silica in the masterbatches is approximately equal to the addition amount of silica (50phr). In
275 contrast, the actual amount of silica in A0K6-MB, A8K0-MB, and A0K0-MB, is obviously lower than
276 the addition amount of silica (50phr). This result further indicates that a huge loss of silica has
277 occurred during coagulation when K-MEPTS or AEO is used individually in silica modification. The
278 results are consistent with the observed macroscopic phenomena in 3.2.1.

279 Because of the interaction between AEO and K-MEPTS, silica modified by using AEO and K-
280 MEPTS together has appropriate chargeability and can be completely co-coagulated with the rubber,
281 which is another key for preparing high performance silica/NR composites by latex compounding
282 method.

283 3.2.3 Micromorphology of the silica/NR masterbatches observed by TEM

284 As shown in Fig. 8, silica can be uniformly dispersed in the matrix without serious aggregation
285 in these masterbatches. The silica dispersion in A6K4-MB is a little bit more homogeneous than in
286 other samples. This composite has fewer silica aggregates than the others. This result demonstrates
287 that the electrostatic attractive force between A6K4-MS and rubber molecule is the most appropriate
288 in these three masterbatches that are successfully prepared.

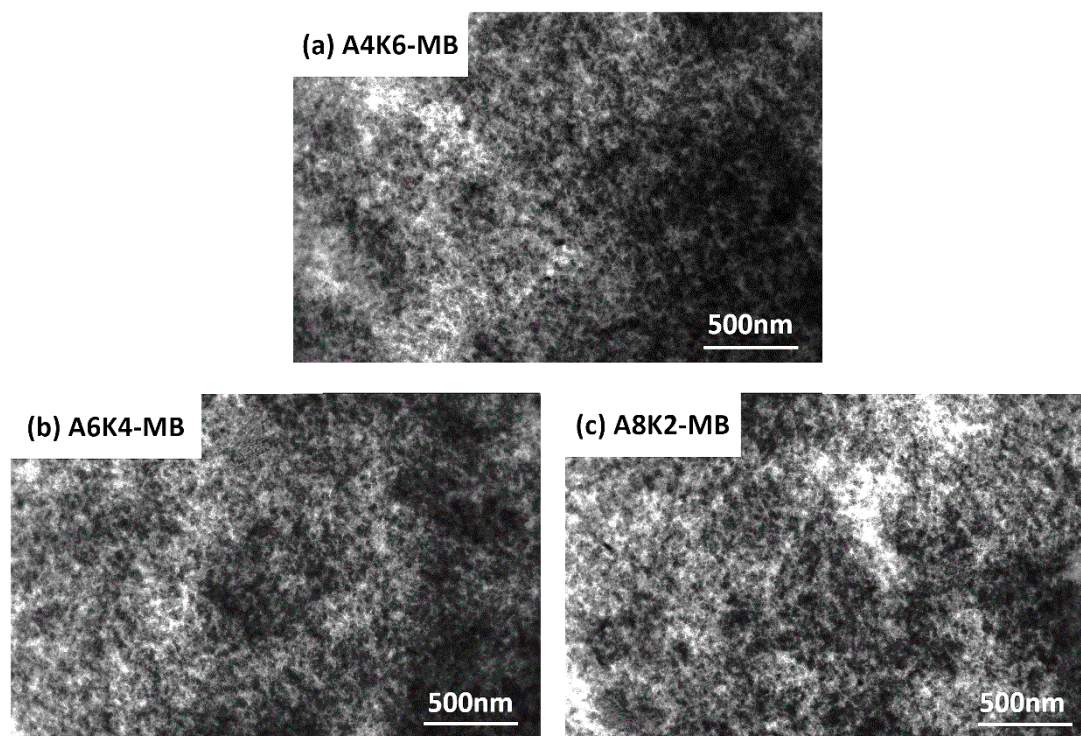


Fig. 8 TEM images of (a) A4K6-MB, (b) A6K4-MB and (c) A8K2-MB

3.3 Characterization of the preparation process of silica/NR composites

The method of preparing A4K6-C, A6K4-C and A8K2-C is described in 2.4. A0K6-C cannot be prepared by use masterbatches because of huge silica loss in preparing A0K6-MB. Therefore, mechanical blending method is used for preparing A0K6-C.

Table 6 Vulcanization characteristics of four kinds of silica/NR compounds

Samples	T ₁₀ /min:sec	T ₉₀ /min:sec	ΔM/ dNm
A0K6-C	0:39	3:02	30.39
A4K6-C	2:03	5:17	28.72
A6K4-C	3:15	5:52	26.89
A8K2-C	3:43	7:20	24.95

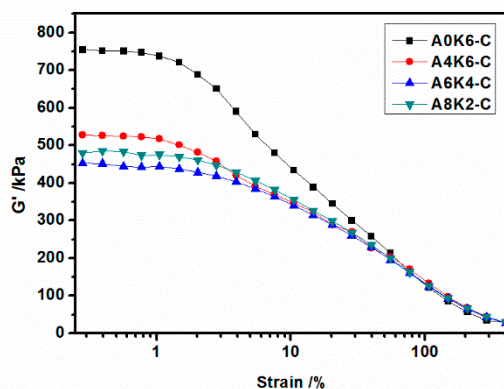
As shown in Table 6, A0K6-C has the shortest scorch time (T₁₀) in all silica/rubber compounds. The scorch time of A4K6-C, A6K4-C, and A8K2-C is longer than that of A0K6-C and increases in turn. The reactivity of mercaptopropyl group decreases when a certain steric hindrance generated by AEO existing. Therefore, AEO has an effect on slowing the rate of reaction between K-MEPTS and rubber. The "scorchy" problem can be mitigated by using AEO and K-MEPTS together in silica modification. Meanwhile, the ΔM of A0K6-C is a little bit more than that of A4K6-C. The silica modified by K-MEPTS could function as a "cross-linking point", resulting in improving crosslinking density of silica/rubber composite, which could be reflected by ΔM. Therefore, AEO has a little effect on preventing the reaction between K-MEPTS and rubber.

3.4 Characterization of silica dispersion in silica/NR composites

3.4.1 Payne effect of silica/NR compounds investigated by RPA

At approximately 1% strain, the G' decreases rapidly with increasing strain and approaches to 0 kPa with sufficiently large strain as shown in Fig. 9. The Payne effect is indicated by the ΔG', which

309 is the difference between the maximum and the minimum G' in the curve [41]. This effect can be
 310 attributed to deformation-induced changes in the microstructure of the material. The Payne effect is
 311 not significant when $\Delta G'$ is small. The low Payne effect indicates high uniformity of the filler
 312 dispersion.

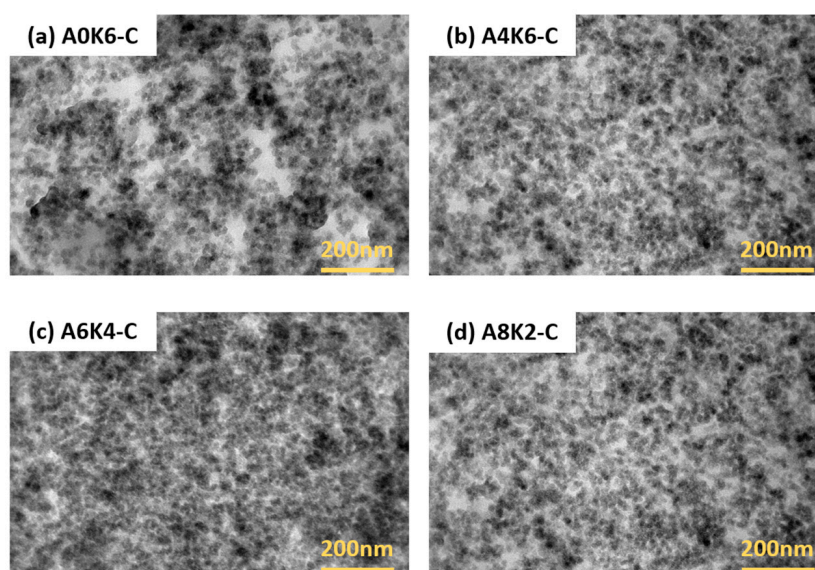


313

314 **Fig. 9** Strain amplitude dependence of the storage modulus (G') of four kinds silica/NR compounds

315 As shown in Fig. 9, A0K6-C exhibits a more obvious Payne effect than other silica/NR
 316 compounds. This finding indicates that the dispersion of silica modified by AEO and K-MEPTS
 317 together in the NR matrix is more homogeneous than that of silica modified by K-MEPTS only in the
 318 same matrix. As indicated in section 3.1.1, AEO could effectively reduce the hydrophilic of silica,
 319 resulting in improving silica dispersion in NR matrix. Meanwhile, the Payne effect of the composite
 320 decreases with the increase of AEO used in silica modification, and then reaches a minimum value
 321 when the weight ratio of AEO to silica is 6:100 and that of K-MEPTS to silica is 4:100 (A6K4-C). This
 322 result shows the same tendency as the silica dispersion in silica/NR masterbatches. Therefore, the
 323 silica dispersion masterbatches directly affects the dispersion of silica in silica/NR compounds, which
 324 further indicates the importance of preparing silica/NR masterbatches with homogeneous silica
 325 dispersion.

326 3.4.2 Micromorphology of the silica/NR composites observed by TEM



327

328

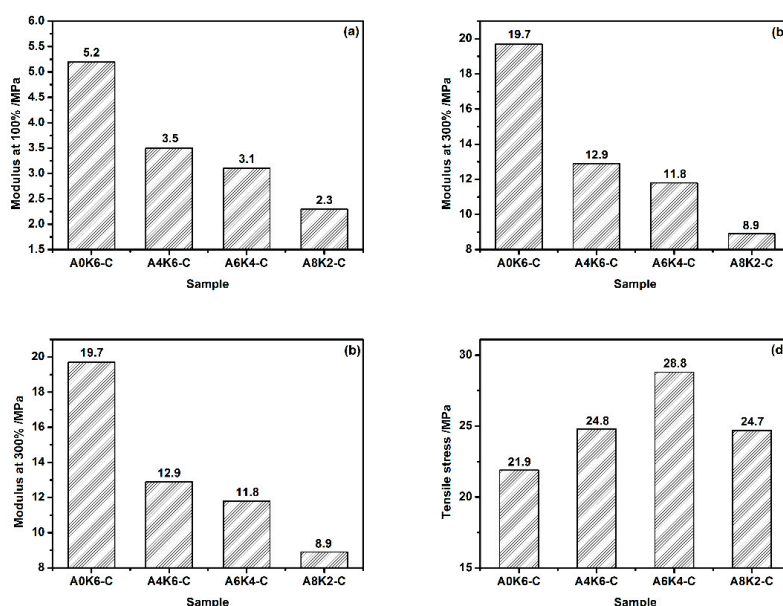
Fig. 10 TEM images of four silica/NR composites

329 As shown in Fig. 10, the silica dispersion in vulcanizates of A4K6-C, A6K4-C and A8K2-C is
 330 significantly more homogeneous than in vulcanizate of A0K6-C, because the latter contains more
 331 silica aggregates. AEO could graft on the silica surface but could not react with rubber, resulting in
 332 forming physical interface between silica and rubber. This physical interface played a role in reducing
 333 the polarity of silica and improving the compatibility between silica and rubber, thus improving the
 334 dispersion of silica in rubber. In contrast, K-MEPTS could graft on the silica surface and react with
 335 rubber, resulting in forming chemical interface between silica and rubber. The silica particles could
 336 be connected with the rubber molecules by the help of K-MEPTS. Therefore, this chemical interface
 337 played a role in preventing the aggregation of primary silica particles. Silica modified by using AEO
 338 and K-MEPTS together could make full use of the advantages of chemical and physical interaction
 339 between silica and rubber. In this research, the silica/NR composites has the best silica dispersion
 340 when the weight ratio of AEO to K-MEPTS is 6:4 in the condition of silica modified by 10% weight
 341 modifiers.

342 3.5 Characterization of silica/NR composites

343 3.5.1 Mechanical performances of silica/NR composites

344 As shown in Fig. 11 (a) and (b), A0K6-C vulcanizate exhibits 50% higher modulus and 40% lower
 345 elongation at break than A4K6-C vulcanizate; meanwhile, the tensile strength of A0K6-C vulcanizate
 346 is 40% lower than that of A4K6-C vulcanizate. The chemical interface formed by K-MEPTS could
 347 function as a “coupling bridge” to improve the reinforcing efficiency of silica on rubber, which was
 348 reflected by a high modulus. However, excessive chemical interface between silica and rubber could
 349 lead to stress-concentrated regions [31], resulting in a low elongation at break. Because of the
 350 physical interface formed by AEO, the most elongated rubber chains could slip along the surface of
 351 silica and equalize the high stress [42], resulting in a proper modulus and elongation at break of
 352 A4K6-C vulcanizate.



353

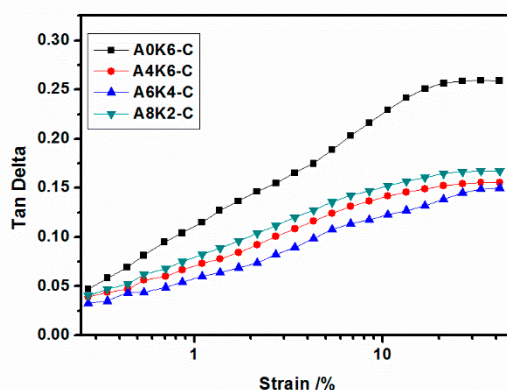
354

355 **Fig. 11** Mechanical performances of silica/NR composites: (a) modulus at 100%, (b) modulus at 100%
 356 elongation, (c) elongation at break and (d) tensile strength

357 For vulcanizates of A4K6-C, A6K4-C and A8K2-C, with decreasing K-MEPTS used in silica
 358 modification, the modulus decreases but the elongation at break increases. The chemical interface
 359 between silica and rubber becomes stronger with the increase of K-MEPTS used in silica modification;
 360 meanwhile, the physical interface between silica and rubber becomes stronger with the increase of
 361 AEO used in silica modification. As presented in Fig. 11 (d), the tensile strength of the composites
 362 has a peak (a value of 28.8 MPa) at the sample of A6K4-C vulcanizate. Tensile strength of silica/NR
 363 composite was affected by both the modulus and the elongation at break. Therefore, mechanical
 364 performances of silica/NR composites are the best, when a proper combination of physical and
 365 chemical interface exists between silica and NR. In this research, the silica/NR composites has the
 366 best mechanical performances when the weight ratio of AEO to K-MEPTS is 6:4 in the condition of
 367 silica modified by 10% weight modifiers.

368 3.5.2 Dynamic performances of silica/NR composites

369 In tire applications, the $\tan \delta$ values at 60 °C are typically used in predicting rolling resistance.



370

371 **Fig. 12** Strain-tan δ curve of four kinds silica/NR composites (60 °C)

372 As presented in Fig. 12, the $\tan \delta$ values at 60 °C in strain from 0.28% to 40% are arranged from
 373 high to low in the following order: A0K6-C vulcanizate, A8K2-C vulcanizate, A4K6-C vulcanizate,
 374 and A6K4-C vulcanizate. The rolling resistance of the A0K6-C vulcanizate is the highest in these four
 375 kinds of silica/NR composite. In theory, the silica fixed with the rubber molecules by chemical
 376 interaction ("coupling bridge") could hardly enhance internal friction loss [4,27]. However, many
 377 silica aggregates were still present in A0K6-C vulcanizate. The mutual friction between silica particles
 378 that were conglutinated tight under cyclic reversed loading was still strong. Therefore, combining a
 379 good silica dispersion and a proper chemical interface between silica and rubber were beneficial to
 380 improve the dynamic performances of silica/NR composites. The physical interface formed by AEO
 381 played a role in improving silica dispersion in rubber matrix. Thus, silica modified by using AEO
 382 and K-MEPTS together could be utilized to improve silica dispersion while silica and rubber are fixed
 383 together.

384 The $\tan \delta$ value of A4K6-C, A6K4-C and A8K2-C vulcanizates is lower than that of A0K6-C
 385 vulcanizate, especially under high strain; moreover, the increase amplitude of their $\tan \delta$ value is low
 386 with increasing strain. A6K4-C vulcanizate has the lowest $\tan \delta$ in all samples, which means that
 387 using A6K4-C composite as tire tread, the rolling resistance of tire minimally changes with increasing
 388 vehicle load. Therefore, using AEO and K-MEPTS is a novel method for preparing silica/NR
 389 composites with excellent dynamic performances. In this research, the silica/NR composites has the
 390 best dynamic performances when the weight ratio of AEO to K-MEPTS is 6:4 in the condition of silica
 391 modified by 10% weight modifiers.

392

393

394 4. Conclusion

395 In this research, latex compounding method was used to prepare high-performance silica/NR
396 composites. Silica is well dispersed in the aqueous phase and can be completely coagulated with the
397 rubber, when silica is modified by using AEO and K-MEPTS together. AEO and K-MEPTS can be
398 grafted on the silica surface simultaneously. Meanwhile, AEO is a more effective modifier than K-
399 MEPTS in changing the hydrophilicity of silica.

400 AEO can generate a certain steric hindrance for the mercaptopropyl group on K-MEPTS,
401 resulting in appropriate chargeability and reactivity for silica modified by using AEO and K-MEPTS
402 together. Therefore, "scorchy" behavior can be solved in this work.

403 AEO and K-MEPTS can form a physical and a chemical interface between silica and rubber,
404 respectively. AEO and K-MEPTS act synergistically to improve the mechanical and dynamic
405 performances of silica/NR composites. In this research, the silica/NR composites has the best
406 mechanical performances when the weight ratio of AEO to K-MEPTS is 6:4 in the condition of silica
407 modified by 10% weight modifiers.

408 Through this study, we can further optimize the preparation of masterbatches using latex
409 compounding method and expand the application range of masterbatches. We hope that the
410 preparation of silica/NR masterbatches by latex compounding method can present practical and
411 profound applications in the rubber industry.

412 **Acknowledgements:** The authors acknowledge financial supports from the National 973 Basic Research
413 Program of China (2015CB654700), the Foundation for Innovative Research Groups of the National Nature
414 Science Foundation of China (51221002 and 51521062), the Major International Cooperation of the National
415 Nature Science Foundation of China (51320105012).

416 Reference

- 417 1. Miloskovska, E.; Nies, E.; Hristova-Bogaerds, D.; van Duin, M.; de With, G. Influence of reaction
418 parameters on the structure of in situ rubber/silica compounds synthesized via sol-gel reaction. *J. Polym.*
419 *Sci., Part B: Polym. Phys.* **2014**, *52*, 967-978.
- 420 2. Dong, B.; Liu, C.; Wu, Y.P. Fracture and fatigue of silica/carbon black/natural rubber composites. *Polym.*
421 *Test* **2014**, *38*, 40-45.
- 422 3. Saeed, F.; Ansarifar, A.; Ellis, R.J.; Haile-Meskel, Y.; Irfan, M.S. Two advanced styrene-
423 butadiene/polybutadiene rubber blends filled with a silanized silica nanofiller for potential use in
424 passenger car tire tread compound. *J. Appl. Polym. Sci.* **2012**, *123*, 1518-1529.
- 425 4. Liu, X.; Zhao, S.H.; Zhang, X.Y.; Li, X.L.; Bai, Y. Preparation, structure, and properties of solution-
426 polymerized styrene-butadiene rubber with functionalized end-groups and its silica-filled composites.
427 *Polymer* **2014**, *55*, 1964-1976.
- 428 5. Hilonga, A.; Kim, J.K.; Sarawade, P.B.; Quang, D.V.; Shao, G.N.; Elineema, G.; Kim, H.T. Synthesis of
429 mesoporous silica with superior properties suitable for green tire. *J. Ind. Eng. Chem.* **2012**, *18*, 1841-1844.
- 430 6. Lin, Y.; Liu, S.Q.; Peng, J.; Liu, L. The filler-rubber interface and reinforcement in styrene butadiene
431 rubber composites with graphene/silica hybrids: A quantitative correlation with the constrained region.
432 *Composites, Part A.* **2016**, *86*, 19-30.
- 433 7. Toyonaga, M.; Chammingkwan, P.; Terano, M.; Taniike, T. Well-defined polypropylene/polypropylene-
434 grafted silica nanocomposites: Roles of number and molecular weight of grafted chains on mechanistic
435 reinforcement. *Polymers* **2016**, *8*, 13.
- 436 8. Sarkawi, S.S.; Dierkes, W.K.; Noordermeer, J.W.M. Elucidation of filler-to-filler and filler-to-rubber
437 interactions in silica-reinforced natural rubber by tem network visualization. *Eur. Polym. J.* **2014**, *54*, 118-
438 127.
- 439 9. Krysztafkiewicz, A.; Binkowski, S.; Jesionowski, T. Adsorption of dyes on a silica surface. *Appl. Surf. Sci.*
440 **2002**, *199*, 31-39.
- 441 10. Iacono, M.; Heise, A. Stable poly(methacrylic acid) brush decorated silica nano-particles by arget atp
442 for bioconjugation. *Polymers* **2015**, *7*, 1427-1443.
- 443 11. Suzuki, N.; Ito, M.; Ono, S. Effects of rubber/filler interactions on the structural development and
444 mechanical properties of nbr/silica composites. *J. Appl. Polym. Sci.* **2005**, *95*, 74-81.
- 445 12. Ramier, J.; Chazeau, L.; Gauthier, C.; Guy, L.; Bouchereau, M.N. Grafting of silica during the processing
446 of silica-filled sbr: Comparison between length and content of the silane. *J. Polym. Sci., Part B: Polym.*
447 *Phys.* **2006**, *44*, 143-152.

- 448 13. Zhang, J.L.; Guo, Z.C.; Zhi, X.; Tang, H.Q. Surface modification of ultrafine precipitated silica with 3-
449 methacryloxypropyltrimethoxysilane in carbonization process. *Colloids Surf., A* **2013**, *418*, 174-179.
- 450 14. Kim, J.H.J.; You, Y.J.; Jeong, Y.J.; Choi, J.H. Stable failure-inducing micro-silica aqua epoxy bonding
451 material for floating concrete module connection. *Polymers* **2015**, *7*, 2389-2409.
- 452 15. Zhang, X.X.; Wen, H.; Wu, Y.J. Computational thermomechanical properties of silica-epoxy
453 nanocomposites by molecular dynamic simulation. *Polymers* **2017**, *9*, 17.
- 454 16. Ridaoui, H.; Donnet, J.B.; Balard, H.; Kellou, H.; Hamdi, B.; Barthel, H.; Gottschalk-Gaudig, T.; Legrand,
455 A.P. Silane modified fumed silicas and their behaviours in water: Influence of grafting ratio and
456 temperature. *Colloids Surf., A* **2008**, *330*, 80-85.
- 457 17. Kunioka, M.; Taguchi, K.; Ninomiya, F.; Nakajima, M.; Saito, A.; Araki, S. Biobased contents of natural
458 rubber model compound and its separated constituents. *Polymers* **2014**, *6*, 423-442.
- 459 18. Wadeesirisak, K.; Castano, S.; Berthelot, K.; Vaysse, L.; Bonfils, F.; Peruch, F.; Rattanaporn, K.;
460 Liengprayoon, S.; Lecomte, S.; Bottier, C. Rubber particle proteins ref1 and srpp1 interact differently
461 with native lipids extracted from hevea brasiliensis latex. *Biochim. Biophys. Acta* **2017**, *1859*, 201-210.
- 462 19. Ibrahim, S.; Daik, R.; Abdullah, I. Functionalization of liquid natural rubber via oxidative degradation
463 of natural rubber. *Polymers* **2014**, *6*, 2928-2941.
- 464 20. Tangpasuthadol, V.; Intasiri, A.; Nuntivanich, D.; Niyompanich, N.; Kiatkamjornwong, S. Silica-
465 reinforced natural rubber prepared by the sol-gel process of ethoxysilanes in rubber latex. *J. Appl. Polym.*
466 *Sci.* **2008**, *109*, 424-433.
- 467 21. Prasertsri, S.; Rattanasom, N. Mechanical and damping properties of silica/natural rubber composites
468 prepared from latex system. *Polym. Test* **2011**, *30*, 515-526.
- 469 22. Gui, Y.; Zheng, J.; Ye, X.; Han, D.; Xi, M.; Zhang, L. Preparation and performance of silica/sbr
470 masterbatches with high silica loading by latex compounding method. *Composites, Part B.* **2016**, *85*, 130-
471 139.
- 472 23. Watanabe, M.; Tamaii, T. Acrylic polymer/silica organic-inorganic hybrid emulsions for coating
473 materials: Role of the silane coupling agent. *J. Polym. Sci. Pol. Chem.* **2006**, *44*, 4736-4742.
- 474 24. Zhou, J.; Zhang, S.W.; Qiao, X.G.; Li, X.Q.; Wu, L.M. Synthesis of sio2/poly(styrene-co-butyl acrylate)
475 nanocomposite microspheres via miniemulsion polymerization. *J. Polym. Sci. Pol. Chem.* **2006**, *44*, 3202-
476 3209.
- 477 25. Li, Y.; Han, B.Y.; Wen, S.P.; Lu, Y.L.; Yang, H.B.; Zhang, L.Q.; Liu, L. Effect of the temperature on surface
478 modification of silica and properties of modified silica filled rubber composites. *Composites, Part A.* **2014**,
479 *62*, 52-59.
- 480 26. Xie, Y.J.; Hill, C.A.S.; Xiao, Z.F.; Militz, H.; Mai, C. Silane coupling agents used for natural fiber/polymer
481 composites: A review. *Composites, Part A.* **2010**, *41*, 806-819.
- 482 27. Li, Y.; Han, B.Y.; Liu, L.; Zhang, F.Z.; Zhang, L.Q.; Wen, S.P.; Lu, Y.L.; Yang, H.B.; Shen, J. Surface
483 modification of silica by two-step method and properties of solution styrene butadiene rubber (ssbr)
484 nanocomposites filled with modified silica. *Compos. Sci. Technol.* **2013**, *88*, 69-75.
- 485 28. Li, Y.; Han, B.; Wen, S.; Lu, Y.; Yang, H.; Zhang, L.; Liu, L. Effect of the temperature on surface
486 modification of silica and properties of modified silica filled rubber composites. *Composites, Part A.* **2014**,
487 *62*, 52-59.
- 488 29. Ostad-Movahed, S.; Yasin, K.A.; Ansarifar, A.; Song, M.; Hameed, S. Comparing effects of silanized
489 silica nanofiller on the crosslinking and mechanical properties of natural rubber and synthetic
490 polyisoprene. *J. Appl. Polym. Sci.* **2008**, *109*, 869-881.
- 491 30. Ansarifar, A.; Wang, L.; Ellis, R.J.; Haile-Meskel, Y. Using a silanized silica nanofiller to reduce excessive
492 amount of rubber curatives in styrene-butadiene rubber. *J. Appl. Polym. Sci.* **2011**, *119*, 922-928.
- 493 31. Gao, Y.Y.; Liu, J.; Shen, J.X.; Cao, D.P.; Zhang, L.Q. Molecular dynamics simulation of the rupture
494 mechanism in nanorod filled polymer nanocomposites. *Phys. Chem. Chem. Phys.* **2014**, *16*, 18483-18492.
- 495 32. Zhang, P.; Zhao, F.; Yuan, Y.; Shi, X.Y.; Zhao, S.G. Network evolution based on general-purpose diene
496 rubbers/sulfur/tbbs system during vulcanization (i). *Polymer* **2010**, *51*, 257-263.
- 497 33. Akbari, A.; Yegani, R.; Pourabbas, B. Synthesis of poly(ethylene glycol) (peg) grafted silica nanoparticles
498 with a minimum adhesion of proteins via one-pot one-step method. *Colloids Surf., A* **2015**, *484*, 206-215.
- 499 34. Cheng, Q.L.; Pavlinek, V.; He, Y.; Lengalova, A.; Li, C.Z.; Saha, P. Structural and electrorheological
500 properties of mesoporous silica modified with triethanolamine. *Colloids Surf., A* **2008**, *318*, 169-174.
- 501 35. Ma, X.K.; Lee, N.H.; Oh, H.J.; Kim, J.W.; Rhee, C.K.; Park, K.S.; Kim, S.J. Surface modification and
502 characterization of highly dispersed silica nanoparticles by a cationic surfactant. *Colloids Surf., A* **2010**,
503 *358*, 172-176.
- 504 36. Wang, W.X.; Li, J.B.; Yang, X.Y.; Li, P.; Guo, C.H.; Li, Q.H. Synthesis and properties of a branched short-
505 alkyl polyoxyethylene ether alcohol sulfate surfactant. *J. Mol. Liq.* **2015**, *212*, 597-604.
- 506 37. Debnath, N.; Mitra, S.; Das, S.; Goswami, A. Synthesis of surface functionalized silica nanoparticles and

- 507 their use as entomotoxic nanocides. *Powder Technol.* **2012**, *221*, 252-256.
- 508 38. Montenegro, L.M.P.; Griep, J.B.; Tavares, F.C.; de Oliveira, D.H.; Bianchini, D.; Jacob, R.G. Synthesis and
509 characterization of imine-modified silicas obtained by the reaction of essential oil of eucalyptus
510 citriodora, 3-aminopropyltriethoxysilane and tetraethylorthosilicate. *Vib. Spectrosc.* **2013**, *68*, 272-278.
- 511 39. Yoshida, T.; Tanabe, T.; Hirano, M.; Muto, S. Ft-ir study on the effect of oh content on the damage process
512 in silica glasses irradiated by hydrogen. *Nucl. Instrum. Methods Phys. Res.* **2004**, *218*, 202-208.
- 513 40. Peng, Z.; Kong, L.X.; Li, S.D.; Chen, Y.; Huang, M.F. Self-assembled natural rubber/silica
514 nanocomposites: Its preparation and characterization. *Compos. Sci. Technol* **2007**, *67*, 3130-3139.
- 515 41. Sajjayanukul, T.; Saeoui, P.; Sirisinha, C. Experimental analysis of viscoelastic properties in carbon
516 black-filled natural rubber compounds. *J. Appl. Polym. Sci.* **2005**, *97*, 2197-2203.
- 517 42. Boonstra, B.B. Mixing of carbon black and polymer: Interaction and reinforcement. *J. Appl. Polym. Sci.*
518 **1967**, *11*, 389-406.

519

520